Available online at www.sciencedirect.com
SCIENCE DIRECT®
Bioorganic & Medicinal Chemistry 13 (2005) 6435–6449
Bioorganic & Medicinal Chemistry

Molecular modeling, design, synthesis, and biological evaluation of novel 3′,4′-dicamphanoyl-(+)-*cis*-khellactone (DCK) analogs as potent anti-HIV agents

Lan Xie,[a,*] Chun-hong Zhao,[a,d] Ting Zhou,[a] Hai-feng Chen,[b,f] Bo-tao Fan,[b] Xian-hong Chen,[a] Jian-zhou Ma,[a] Jing-yun Li,[c] Zhuo-yi Bao,[c] Zhaowen Lo,[d] Donglei Yu[e] and Kuo-Hsiung Lee[e]

[a]*Beijing Institute of Pharmacology and Toxicology, Beijing 100850, China*
[b]*ITODYS CNRS-UMR7086, University Paris 7-Denis Diderot, 1 Rue Guy de la Brosse, 75005 Paris, France*
[c]*Beijing Institute of Microbiology and Epidemiology, Beijing 100850, China*
[d]*Department of Chemistry, Hubei University, Wuhan, Hubei 430062, China*
[e]*Natural Products Laboratory, School of Pharmacy, University of North Carolina at Chapel Hill, Chapel Hill, NC 27599, USA*
[f]*Laboratory of Computer Chemistry, Shanghai Institute of Organic Chemistry, Shanghai, 200032, China*

Received 12 April 2005; accepted 30 June 2005
Available online 2 August 2005

Abstract—Our current studies aimed at developing new potential anti-AIDS drug candidates have focused on the design and synthesis of new DCK analogs with improved molecular water solubility. Based on the structures and biodata of previous DCK analogs, 3D-QSAR studies have been performed which resulted in two reliable computational models, CoMFA and CoMSIA, with r^2 values of 0.995 and 0.987, and q^2 values of 0.662 and 0.657, respectively. In accord with these 3D-QSAR models, 15 new DCK analogs with polar functional groups at the 3-position were subsequently designed, synthesized, and evaluated against HIV-1 replication in H9 and MT4 cell lines. New DCK analogs **3b**, **3c**, **4b**, **4c**, **6a**, **7c**, and **9a** showed promising potency with EC_{50} values ranging from 0.09 to 0.0002 μM in both assays. Meanwhile, these promising compounds also showed a wide range of predicted log *P* values from 0.90 to 5.19, which increased the probability of identifying anti-HIV drug candidates from this class of compounds for clinical trials. Furthermore, both experimental and predicted values matched well, corroborating the reliability of the established 3D-QSAR models.

1. Introduction

With ca. 42 million HIV/AIDS patients worldwide, only 20 anti-HIV drugs are currently available for clinical use. These anti-HIV drugs include reverse transcriptase (RT) inhibitors, protease inhibitors, and fusion inhibitors. They can be used alone or as part of a combination regimen to treat HIV infection and AIDS patients. However, in the course of time HIV has developed resistance to all currently available drugs, which has rapidly brought down the efficiency of these medicines. Therefore, new anti-HIV agents with novel structures or mechanism(s) of action are in demand to tackle this problem.

In our previous research, 3′,4′-di-*O*-(*S*)-camphanoyl-(+)-*cis*-khellactone (DCK, **M01**) displayed better potency than AZT against HIV replication in H9 lymphocytes,[1] and was identified as a potent anti-HIV agent. Subsequently, DCK was systematically modified, and more than 100 khellactone derivatives including mono- and di-substituted DCK analogs were synthesized and evaluated against HIV-1 replication in H9 lymphocytes.[2] The SAR studies[3–5] have shown that essential structural moieties of DCK analogs for anti-HIV activity are the following: (1) the 3′*R*, 4′*R* absolute configurations, (2) planarity of the coumarin nucleus, (3) a methyl group at the 4-position, and (4)

* Corresponding author. Fax: +1 919 966 3893; e-mail: khlee@email.unc.edu

0968-0896/$ - see front matter © 2005 Elsevier Ltd. All rights reserved.
doi:10.1016/j.bmc.2005.06.057

two bulky groups at the 3′- and 4′-positions. In addition, the 3-, 4-, and 5-positions on the coumarin ring are all modifiable by introducing an alkyl or alkoxy group. The mechanism of action studies have demonstrated that active DCK analogs inhibit the production of double-stranded viral DNA from a single-stranded DNA intermediate,[6] in stark contrast to current HIV-RT inhibitors that block the generation of single-stranded DNA from the RNA template. These exciting results strongly motivated us to develop these studies to the drug development stage. On account of its high potency and efficient synthesis, 4-methyl-DCK (**M02**)[7] was then chosen as a drug candidate for preclinical studies. However, low solubility and poor bioavailability of **M02** restricted its further development. Therefore, our research turned again to studying the novel modification of DCK analogs to explore and identify new drug candidates with potent anti-HIV activity and desirable pharmaceutical properties.

Based on our previous work that dealt with the theoretical study of non-nucleoside RT inhibitors,[8] we carried out molecular modeling analyses that were based on the structures and anti-HIV data of known DCK analogs, and established two 3D-QSAR models, CoMFA and CoMSIA, to guide further structural optimization and predict the potency and physicochemical properties of clinical drug candidates. Subsequently, several newly designed DCK analogs have been synthesized and evaluated for anti-HIV activity in both H9 and MT-4 cell lines. This paper reports our new results.

2. Molecular modeling

2.1. Methods and data set for analysis

CoMFA and CoMSIA are now established tools for building 3D-QSAR models that can be applied to drug design.[9,10] Accordingly, we used the structures of 21 DCK analogs and their anti-HIV activities (EC_{50} in μM) in H9 lymphocytes (Table 1A) to establish CoMFA and CoMSIA models in the present study. Seventeen structures constituted a training set and all molecules

Table 1A. Structures of DCK analogs and their biodata (EC_{50} and pEC_{50}) in H9 lymphocytes

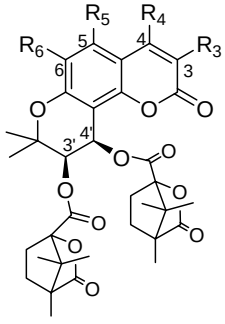

Compound	Structure	EC_{50} (μM)[a]	pEC_{50}
M01	DCK[b](R_3=R_4=R_5=R_6=H)	0.04900	1.31
M02	4-Me-DCK[c]	0.00594	2.23
M03	5-MeO-4-Me-DCK	—	—
M04*	3-Me-DCK	0.02731	1.56
M05	5-Me-DCK	0.00600	2.22
M06	4,5-di-Me-DCK	0.12000	0.92
M07	4,6-di-Me-DCK	0.05800	1.24
M08	3-OMe-DCK	0.01043	1.98
M09*	4-OMe-DCK	0.05106	1.29
M10	5-OMe-DCK	0.04387	1.36
M11	3-Cl-4-Me-DCK	0.00075	3.12
M12	3-CH_2Br-DCK	0.05942	1.23
M13	3-CH_2OAc-DCK	0.06767	1.17
M14	3-CH_2OH-DCK	0.03466	1.46
M15*	3-CH_2NH_2-DCK	0.67658	0.17
M16	3-CH_2NEt_2-DCK	3.67398	−0.57
M17	4-Me-3-CH_2OAc-DCK	0.02800	1.55
M18	6-CH_2OH-4-Me-DCK	0.11100	0.95
M19	4-Me-3-CH_2OH-DCK	0.01622	1.79
M20	3-$CHBr_2$-DCK	0.94916	0.02
M21	4-Me-6-CH_2Br-DCK	0.02462	1.61
M22*	4-Me-3-CH_2Br-DCK	0.00741	2.13

[a] All EC_{50} data presented in the table are averages of at least two separate experiments performed by Panacos Pharmaceuticals, Inc.
[b] $EC_{50} = 2.56 \times 10^{-4}$ μM in previous screenings and publications.[1]
[c] $EC_{50} = 1.83 \times 10^{-6}$ in previous screenings and publication.[7]

Table 1B. Structures, EC_{50} values in H9 lymphocytes, and calculated pEC_{50} of DCP analogs[21]

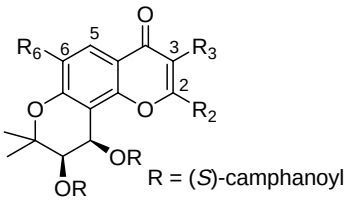

Compound	Structure	EC_{50}(μM)	pEC_{50}
M23*	$R_2 = CH_2CH_2CH_3$, $R_3 = R_6$=H	0.02	1.70
M24*	$R_2 = CH(CH_3)_2$, $R_3 = R_6$ = H	0.07	1.15
M25*	$R_2 = CH_2OCH_2CH_3$, $R_3 = R_6$ = H	0.10	1.00
M26*	R_2 = ph, $R_3 = R_6$ = H	0.13	0.89
M27*	$R_2 = CH_2CH_3$, R_3 = H, R_6 = *t*-Bu	1.62	−0.21

in the test set have been denoted as '*'. Five DCP {3′*R*,4′*R*-di-*O*-(*S*)-camphanoyl-2′,2′-dimethyl-dihydropyrano[2,3-*f*]chromone} compounds (Table 1B), which are structurally similar to the DCK analogs, were also used in the test set. Three-dimensional structure building and all the modeling were carried out using the SYBYL[11] program package, and conformations of compounds in the training and test sets were generated using the multi-search method implemented in SYBYL. Energy minimization was effected using the Tripos force field[12] with a distance-dependent dielectric and the Powell conjugate gradient algorithm with a convergence criterion of 0.01 kcal/(mol Å). Partial atomic charges were calculated using the Gasteiger–Hückel method.

Cross-validated q^2 usually serves as the quantitative measurement for the prediction of CoMFA and CoMSIA. However, Cho and Tropsha[13] have reported that the q^2 value is sensitive to the orientation of aligned molecules on the computer terminal and, thus, might vary with the orientation by as much as 0.5 q^2 units. Therefore, suitable alignment rules must be framed while constructing 3D-QSAR models. Consequently, the DCK compounds in Tables 1A and 1B were aligned according to their common substructure (the three fused rings of the DCK skeleton), and compound **M02** (Table 1A), one of the most promising analogs in the H9 lymphocyte screening assay, was used as the alignment template. Molecular alignment was effected with the routine SYBYL function of 'database align'.

2.2. CoMFA models

After consistently aligning the molecules within a lattice that extended 4 Å units beyond the aligned molecules in all directions with a grid step size of 2 Å, a probe sp^3 carbon atom with +1 net charge was employed. Steric and electrostatic interactions between the probe and the remaining molecules were calculated. The generated steric and electrostatic fields were scaled by the CoMFA-STD method in SYBYL with a default energy of 30 kcal/mol. Electrostatic interactions were modeled using a Coulomb potential and van der Waals interactions using a Lennard-Jones potential. The regression analysis was carried out using the partial least-squares (PLS)[14] method. The final model was developed with an optimum number of components yielding the highest q_{cv}^2. The total set of inhibitors was initially divided into two groups in an approximate ratio of 2:1 (for example, 17 in training set to 9 in the test set). Test set and training set compounds were selected manually such that low, moderate, and high activity compounds were present in roughly equal proportions in both sets.

2.3. CoMSIA models

CoMSIA similarity indices were derived with the method proposed by Klebe and co-workers,[15,16] with the same lattice box as that used for the CoMFA calculations. Five physicochemical properties, such as steric, electrostatic, hydrophobic, hydrogen bond donor, and hydrogen bond acceptor fields, were evaluated on the probe atom. Gaussian-type distance dependence was studied to measure the relative attenuation of the field position of each atom in the lattice. The use of Gaussian-type distance dependence in CoMSIA led to much smoother sampling of the fields around the molecules when compared to CoMFA. A default value of 0.3 was used as the attenuation factor.

2.4. Regression analysis

To derive 3D QSAR models, the CoMFA and CoMSIA descriptors were used as independent variables and the pEC_{50} activity value as a dependent variable. Partial least-squares (PLS) regression analyses were conducted with standard implementation in the SYBYL package. The predictive values of the models were evaluated by leave-one-out (LOO) cross-validation. The cross-validated coefficient, q^2, was calculated using Eqs. 1 and 2.[17]

$$q^2 = 1 - \frac{\mathrm{PRESS}}{\sum_{i=1}^{N}(y_i - y_\mathrm{m})^2}, \tag{1}$$

$$\mathrm{PRESS} = \sum_{i=1}^{N}(y_{\mathrm{pred},i} - y_i)_2, \tag{2}$$

where y_i is the activity for training set compounds, y_m is the mean observed value, corresponding to the mean of

the values for each cross-validation group, and $y_{pred,i}$ is the predicted activity for y_i.

2.5. 3D-QSAR model

Two methods, CoMFA and CoMSIA, were used to construct 3D-QSAR models for DCK analogs. The statistical parameters of the models are given in Table 2. The predicted activities and the residuals between experimental (EA) and predicted (PA) activities are listed in Tables 3 and 4.

2.6. Selection of CoMSIA fields

In optimizing CoMSIA performance, the most important parameter is how to combine the five fields in a CoMSIA model. To select the optimal result, we systemically changed the combination of fields and chose that value which gave the best non-cross validation, smallest errors, and the largest F value. Figure 1 shows the detailed results. Finally, the model generated by combining the steric, electrostatic, hydrophobic, and hydrogen bond acceptor fields was chosen as the best CoMSIA model, and the contours were analyzed using this model.

2.7. Evaluation of CoMFA and CoMSIA models

We next studied the correlation models between experimental and predicted anti-HIV activities obtained with SYBYL 6.9.

For the CoMFA model, the cross-validated q^2 value of the training set was 0.662, with six principal components. The non-cross-validated r^2 value was 0.995, with standard error (SE) 0.075. Four structurally diverse DCK compounds and five additional DCP analogs, which were not included in the CoMFA and CoMSIA models, were selected as a validation set. The corresponding correlation coefficient r^2 between EA and PA for the test set was 0.900, with standard error (SE) 0.254. The correlations between EA and PA for training and test sets are shown in Figure 2. These results confirm the good prediction ability of this 3D model.

For the CoMSIA (SEHA) model, the cross-validated q^2 value of training set was 0.657, with six principal components. The non-cross-validated r^2 value was 0.987, with standard error (SE) 0.119. The corresponding correlation coefficient r^2 between EA and PA for test

Table 2. PLS statistics of CoMFA and CoMSIA 3D-QSAR models

PLS statistics	CoMFA				CoMSIA				
	SE	SE	SHE	SED	SEA	SEDA	SEHD	SEHA	SEHDA
q^2	0.662	0.739	0.668	0.579	0.666	0.588	0.614	0.657	0.618
R^2	0.995	0.981	0.986	0.973	0.972	0.964	0.977	0.987	0.977
S	0.075	0.146	0.125	0.175	0.178	0.200	0.159	0.119	0.159
F	333.355	85.805	117.839	59.176	57.167	45.226	71.756	131.133	71.975
PLS components	6	6	6	6	6	6	6	6	6
Steric	0.576	0.354	0.208	0.337	0.275	0.267	0.203	0.173	0.176
Electrostatic	0.424	0.646	0.385	0.592	0.407	0.380	0.363	0.277	0.268
Hydrophobic	—	—	0.408	—	—		0.389	0.323	0.307
Donor	—	—	—	0.071	—	0.063	0.045	—	0.042
Acceptor	—	—	—	—	0.317	0.290	—	0.227	0.207

S = steric field, E = electrostatic field, H = hydrophobic field, D = hydrogen bond donor, A = hydrogen bond acceptor.

Table 3. The experimental and predicted activities of training sets

Compound	pEC_{50}	CoMFA		CoMSIA (SEHA)	
		PA	Res.	PA	Res.
M01	1.31	1.304	0.01	1.196	0.11
M02	2.23	2.195	0.03	2.141	0.09
M05	2.22	2.203	0.02	2.131	0.09
M06	0.92	0.967	−0.05	1.098	−0.18
M07	1.24	1.216	0.02	1.255	−0.02
M08	1.98	1.996	−0.01	1.947	0.03
M10	1.36	1.340	0.02	1.308	0.05
M11	3.12	3.141	−0.02	3.077	0.05
M12	1.23	1.382	−0.16	1.431	−0.20
M13	1.17	1.184	−0.01	1.206	−0.04
M14	1.46	1.541	−0.08	1.545	−0.08
M16	−0.57	−0.561	0.00	−0.673	0.11
M17	1.55	1.455	0.10	1.537	0.02
M18	0.95	0.948	0.01	0.879	0.08
M19	1.79	1.699	0.09	1.795	0.00
M20	0.02	−0.014	0.04	0.049	−0.03
M21	1.61	1.608	0.00	1.682	−0.07

Table 4. The experimental and predicted activities of test sets

Compound	pEC_{50}	CoMFA		CoMSIA(SEHA)	
		PA	Res.	PA	Res.
M04	1.56	1.581	−0.02	1.644	−0.08
M09	1.29	1.345	−0.05	1.375	−0.08
M15	0.17	0.079	0.09	0.122	0.05
M22	2.13	2.270	−0.14	2.215	−0.08
M23	1.70	1.72	−0.02	1.74	−0.04
M24	1.15	1.13	0.02	1.14	0.01
M25	1.00	1.04	−0.04	0.94	0.06
M26	0.89	0.89	0.00	0.91	−0.02
M27	−0.21	0.49	−0.70	0.33	−0.54

set was 0.942, with standard error (SE) 0.198. The correlations between EA and PA for training and test sets are shown in Figure 3. The residues for all tested compounds (except for **M27**) were less than 0.08, indicating that this CoMSIA model has good prediction ability.

Therefore, these models (CoMFA and CoMSIA) could be used to design new anti-HIV compounds.

2.8. Analysis of CoMFA and CoMSIA models

From Table 2, the contributions of steric and electrostatic fields in the CoMFA model are 0.576 and 0.424, respectively. Figure 4 shows the contour plots of this model with structure **M02**. The interpretations ascribed to different colors are given in the legend. Yellow and red regions near the C-3 substituent suggest that small

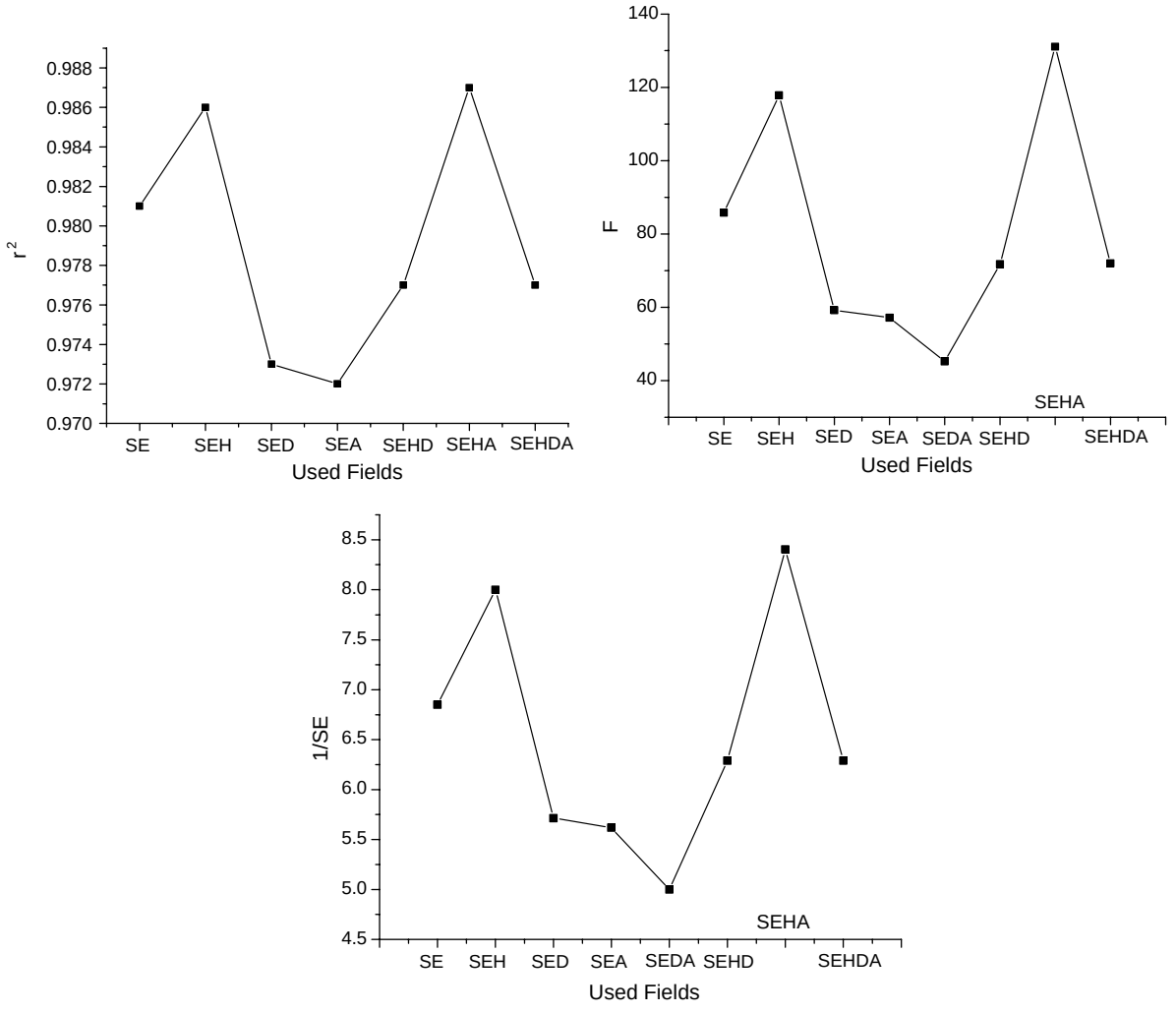

Figure 1. The influence of combined fields.

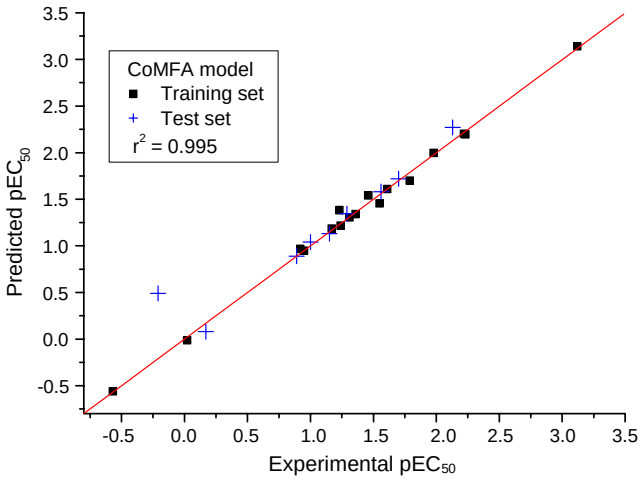

Figure 2. Correlations between PA and EA of a CoMFA Model.

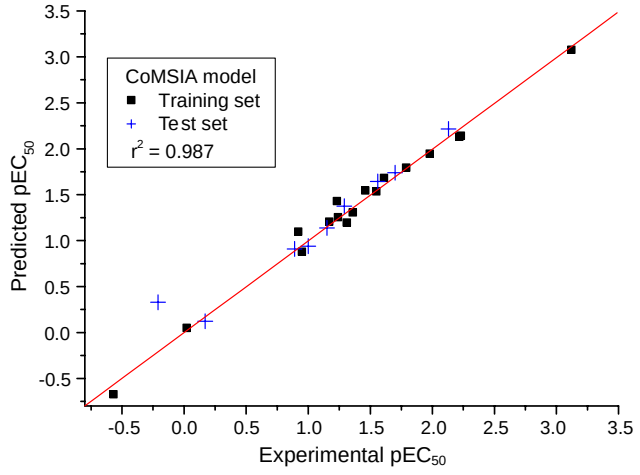

Figure 3. Correlations between PA and EA of CoMSIA Model.

and electronegative groups at this position, respectively, should favor anti-HIV activity. The experimental results agreed with these CoMFA results, as compounds **M16** and **M20** with bulky substituents at this position show low activity, while compounds **M11** (3-Cl) and **M22** (3-CH_2Br) with electronegative groups have high inhibitory potency. Both green and yellow regions near the 4-position show that substituents with suitable volumes will be favorable to activity.

The contributions of steric, electrostatic, hydrophobic, and hydrogen bond acceptor fields in the CoMSIA model are 0.173, 0.277, 0.323, and 0.227, respectively. The contour plots with structure **M02** are illustrated in Figure 5. Yellow, red, magenta, cyan, and white regions near the substituent at the 3-position suggest that suitable hydrophobic, small, electronegative, and hydrogen bond donor groups, respectively, are favorable to activity. These findings complement those of the CoMFA model and explain the high activities of **M13**, **M14**, **M17**, and **M19**. The same observations are valid for the DCP analogs.

2.9. Design of new compounds

Because high hydrophobicity might be one reason for the failure of the first-generation active DCK analogs as drug candidates, our continuing studies have aimed at improving molecular water solubility and at potentially enhancing molecular absorption and oral bioavailability. Guided by the above CoMFA and CoMSIA models and known pharmacophores, novel structural modification focused on the 3-substituents. Accordingly, we synthesized mono- (c series), di- (b series), and tri-substituted (a series) DCK analogs with 3-nitromethyl (CH_2NO_2), 3-cyanomethyl (CH_2CN), 3-methylcarbamate (CH_2OCONH_2), 3-hydroxymethyl (CH_2OH), and 3-halide (X) moieties to explore better drug candidates for clinical trial. Because 4-methyl-DCK (**M02**) and 4-methyl-5-methoxy-DCK (**M03**) are the most potent first-generation DCK analogs,[5] they served as leads for the current di- (b series) and tri-substituted (a series) DCK analogs, respectively. New trisubstituted compounds **2a**, **5a**, and **6a** could be readily compared with previously prepared active mono- and di-substituted analogs. With a C-5 methoxy group, the trisubstituted DCKs would have lower log *P* values than the corresponding mono- and di-substituted DCKs (Table 5), but would also involve more synthetic steps.

As shown in Table 5, the 3D-QSAR models predicted that all of the newly designed compounds would be

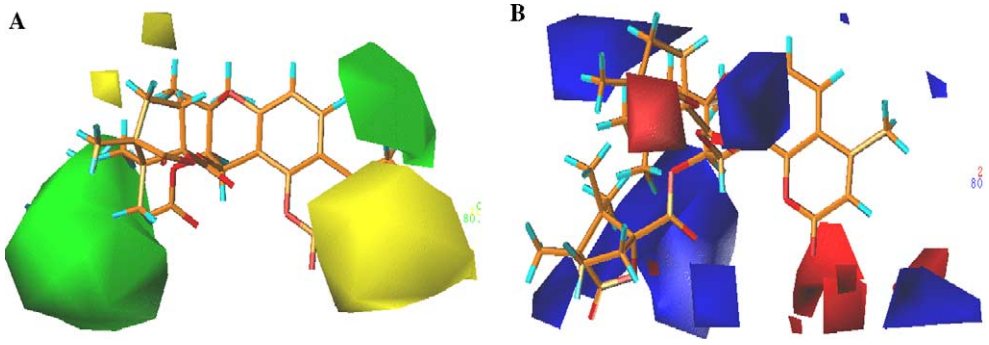

Figure 4. CoMFA contour plots. (A, steric field, B, electrostatic field) Green contours indicate regions where bulky groups are favorable to activity, whereas yellow contours indicate regions where bulky groups are not desirable for activity. Blue contours indicate regions where the positive groups could increase activity, whereas red contours indicate the regions needing negative charge.

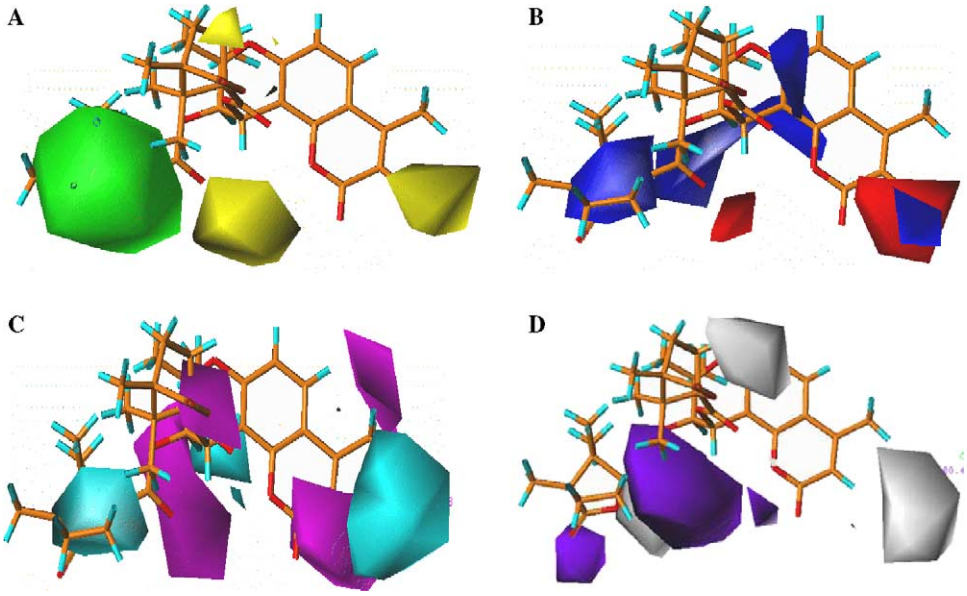

Figure 5. CoMSIA contour plots. (A, steric field; B, electrostatic field; C, hydrophobic field) Magenta contours indicate regions where hydrophobic groups are favorable to activity, whereas cyan contours indicate regions where hydrophilic groups are favorable to activity. D, hydrogen bond acceptor field (purple contours indicate regions where hydrogen bond acceptor groups are favorable to activity, whereas white contours indicate regions where hydrogen bond donor groups are favorable to activity).

Table 5. Predicted pEC_{50} (CoMFA and CoMSIA) and log *P* values of new DCK analogs

Compound	Structure	CoMFA	CoMSIA	log *P*
2a	3-CH_2Br-4-Me-5-OMe-DCK	0.326	0.453	5.32
M22	3-CH_2Br-4-Me-DCK[a]	2.270	2.215	5.58
M12	3-CH_2Br-DCK[a]	1.382	1.431	5.42
3a	3-CH_2NO_2-4-Me-5-OMe-DCK	0.576	0.767	0.80
3b	3-CH_2NO_2-4-Me-DCK	1.663	1.803	1.06
3c	3-CH_2NO_2-DCK	1.407	1.835	0.90
4a	3-CH_2CN-4-Me-5-OMe-DCK	0.924	0.849	4.94
4b	3-CH_2CN-4-Me-DCK	1.622	1.745	5.19
4c	3-CH_2CN-DCK	1.778	1.649	5.04
5a	3-CH_2OAc-4-Me-5-OMe-DCK	0.016	0.002	4.24
M17	3-CH_2OAc-4-Me-DCK[a]	1.455	1.537	4.50
M13	3-CH_2OAc-DCK[a]	1.184	1.206	4.34
6a	3-CH_2OH-4-Me-5-OMe-DCK	2.246	1.883	4.11
M19	3-CH_2OH-4-Me-DCK[a]	1.006	1.160	4.37
M14	3-CH_2OH-DCK[a]	1.541	1.545	4.21
7b	3-CH_2OCONH_2-4-Me-DCK	0.464	1.065	3.95
7c	3-CH_2OCONH_2-DCK	1.209	0.948	3.80
8a	3-Cl-4-Me-5-OMe-DCK	0.754	0.184	4.74
M11	3-Cl-4-Me-DCK[a]	3.141	3.077	4.99
9a	3-F-4-Me-5-OMe-DCK	0.453	0.246	4.36
9b	3-F-4-Me-DCK	2.305	1.047	4.61

[a] Compounds published previously for comparison.

active against HIV replication. Their log *P* values were also calculated with HYPERCHEM 7.0. From these calculations, we could observe that changes in the 3-substituents resulted in the formation of new compounds with a wide range of log *P* values, from 0.8 to 5.58, which included both H-bond acceptors and donators. The molecular log *P* values followed a decreasing order of NO_2 > $OCONH_2$ > OH > OAc > F > Cl > H > CN > Br. In general, log *P* values of <5 are of benefit to improve molecular water solubility and enhance oral bioavailability and, thus, are sought after in potential drug compounds. However, although their calculated log *P* values were >5, 3-cyanomethyl-DCK (**4c**) and 3-cyanomethyl-4-methyl-DCK (**4b**) were predicted to be very potent against HIV replication. Hence, synthesis and biological evaluation of both compounds may provide meaningful information for QSAR validation and analog design.

3. Chemistry

As shown in Scheme 1, our syntheses began with methylated DCKs (**1a**–**1c**), which were synthesized from

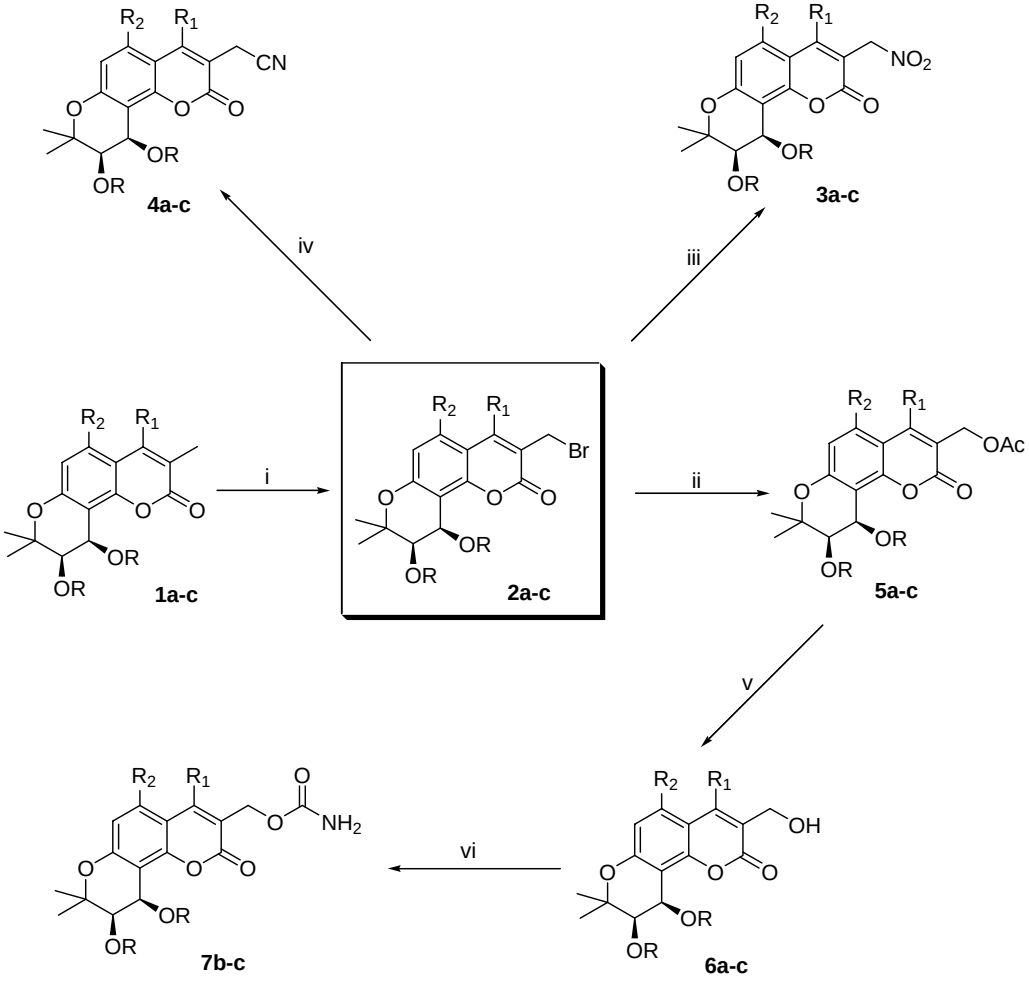

Scheme 1. Synthesis of new DCK analogs. Reagents and conditions: (i) NBS, benzene; (ii) $NaOAc/Ac_2O$, reflux; (iii) $NaNO_2$, DMF; (iv) NaCN, DMSO; (v) 10% HCl aq/EtOH, reflux; (vi) 1—*p*-nitrophenyl chloroformate, CH_2Cl_2; 2—NH_3

corresponding methylated 7-hydroxycoumarins, as previously described. 3-Methylated compounds (**1a**–**1c**) were treated with *N*-bromosuccinimide at a molar ratio of 1:1 in refluxing anhydrous benzene to produce 3-bromomethyl-substituted DCKs (**2a**–**2c**) in 67–77% yield. Where both 3- and 4-methyl groups were present, bromination occurred exclusively at the former based on NMR shifts and NOE measurements. The 3-bromomethyl substituent was then converted to different functional groups. When treated with sodium nitrite or sodium cyanide, the 3-bromomethyl compounds were converted to the corresponding 3-nitromethyl (**3a**–**3c**) and 3-cyanomethyl (**4a**–**4c**) analogs, respectively. The 3-bromomethyl-DCK derivatives were also reacted with acetic anhydride in the presence of sodium acetate to provide the corresponding 3-acetoxymethyl-DCK derivatives (**5a**–**5c**). Acidic hydrolysis then gave the corresponding 3-hydroxymethyl-DCKs (**6a**–**6c**). Reaction with *p*-nitrophenyl chloroformate, followed by treatment with aqueous NH_3, produced the corresponding 3-carbamoyloxymethyl-DCKs (**7b** and **7c**).[18]

3,4-Dimethyl-5-methoxy-DCK (**1a**), 3-fluoro-5-methoxy-4-methyl-DCK (**8a**), and 3-chloro-5-methoxy-4-methyl-DCK (**9a**) were synthesized from 7-methoxy-2,2-dimethyl-5-hydroxy-4-chromanone (**23**),[5] as shown in Scheme 2. The 4-carbonyl group in **23** was readily reduced to a methylene with $NaBH_4$ in refluxing THF solution under basic conditions. Then, the lactone ring was cyclized by a Pechmann reaction with ethyl 2-methylacetoacetate, ethyl 2-chloroacetoacetate, or ethyl 2-fluoroacetoacetate using boron trifluoride diethyl etherate as a catalyst to afford trisubstituted dihydroseselins **24**, **25**, and **26**, respectively, in >50% yield. Compounds **24**–**26** were dehydrogenated with DDQ in dioxane or THF at reflux to yield the corresponding trisubstituted seselins **27**–**29**.[19] As shown in Scheme 3, intermediate 3-fluoro-4-methylseselin (**31**) was also synthesized from 1,3-benzenediol by the Pechmann reaction with ethyl 2-fluoroacetoacetate, followed by nucleophilic substitution with 3-chloro-3-methylbut-1-yne under basic conditions, and then Claisen thermal rearrangement. Finally, Sharpless asymmetric dihydroxylation, followed

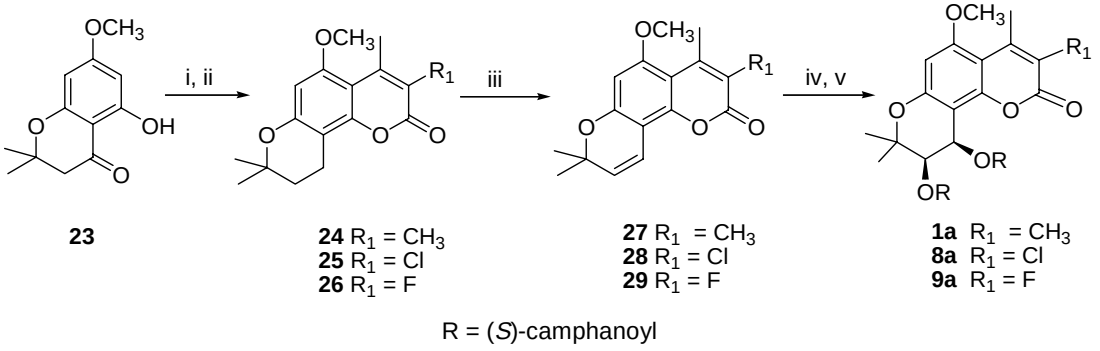

Scheme 2. Synthesis of DCK analogs **1a**, **8a**, and **9a**. (i) $NaBH_4$/toluene; (ii) $CH_3COCHR_1CO_2C_2H_5$; (iii) DDQ; (iv) $K_3Fe(CN)_6$, K_2CO_3, $(DHQ)_2$–Pyr, $K_2Os_2(OH)_4$, *t*-BuOH/H_2O (v/v=1/1), ice bath; (v) (*S*)-camphanic chloride, CH_2Cl_2/Py

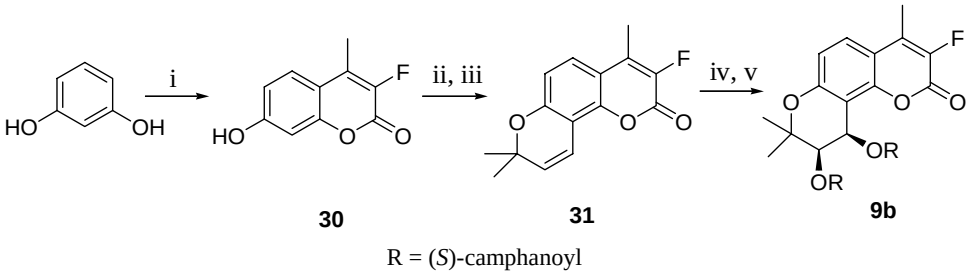

Scheme 3. Synthesis of DCK analog **9b**. Reagents and conditions: (i) ethyl 2-fluoroacetoacetate/H_2SO_4; (ii) 3-chloro-3-methyl-1-butyne/DMF/K_2CO_3/KI; (iii) *N*,*N*-diethylaniline, reflux; (iv) $K_3Fe(CN)_6$, K_2CO_3, $(DHQ)_2$–Pyr, $K_2Os_2(OH)_4$, *t*-BuOH/H_2O (v/v 1/1), ice bath; (v) (*S*)-camphanic chloride, CH_2Cl_2/Py

by acylation with (*S*)-camphanoyl chloride, gave trisubstituted DCK analogs **1a**, **8a**, **9a**, and 3-fluoro-4-methyl-DCK (**9b**), respectively, based on methods described previously.[20] The percent diastereomeric excess (% de) of all chiral target DCKs was determined from their ^1H NMR spectra.

4. Results and discussion

The 14 newly synthesized DCKs were tested in parallel with AZT against HIV-1 replication in acutely infected H9 lymphocytes and the MT-4 cell line, and the data are shown in Table 6. All new target DCKs exhibited potent inhibitory activities against HIV replication in this assay with EC_{50} values <1.95 μM. The most promising compounds were mono- and di-substituted 3-cyanomethyl-DCK analogs **4c** and **4b** with EC_{50} values of 0.0002 and 0.0024 μM, and a remarkable selectivity index (SI) of >189,100 and >15,433, respectively. Both compounds were not only more potent than AZT in the same assay, but were also much more active than their predicted potency (Table 7). Another pair of mono- and di-substituted 3-nitromethyl-DCKs (**3c** and **3b**) also exhibited potent anti-HIV activity (EC_{50} = 0.0288 and 0.0230 μM, respectively). However, with EC_{50} values of 0.11 and 0.27 μM, the corresponding trisubstituted DCKs **4a** and **3a** were less potent than the related di- or mono-substituted DCKs (**4b–c** and **3b–c**). Furthermore, the mono-substituted 3-carbamoyloxymethyl-DCK (**7c**), the trisubstituted 3-hydroxymethyl-5-methoxy-4-methyl-DCK (**6a**), and 3-fluoromethyl-5-methoxy-4-methyl-DCK (**9a**) also exhibited potent anti-HIV activity with EC_{50} values of 0.0777, 0.0522, and 0.0175 μM, respectively.

All new compounds, except for **9b**, were also evaluated in the MT-4 cell line. Except for **5a**, which was inactive in this assay, the remaining compounds exhibited potent anti-HIV activity with EC_{50} values <5.45 μM. Interestingly, **6a**, the most promising compound in the MT-4 cell line assay (EC_{50} = 0.00129 μM, SI = >55,690) was more potent than in H9 lymphocytes. With this exception, the compounds were generally less potent in the MT-4 cell line than in H9 lymphocytes, because the MT-4 cell line is less sensitive than H9 lymphocytes. However, both assays showed similar activity patterns and confirmed the anti-HIV activities of the newly designed DCK analogs.

Finally, the experimental EC_{50} results in the H9 assay were converted to pEC_{50} values and compared with those predicted by the CoMFA and CoMSIA models. The comparisons are given in Table 7. While compounds **4b**, **4c**, and **9a** were more potent than predicted, it was encouraging to find that most experimental data matched well with the predicted potency. Therefore, the current bioassay data strongly supported the reliability of the developed 3D-QSAR models.

In addition, with a wide log *P* range from 1 to 5, the current potent DCKs provide a better selection of drug candidates with suitable molecular ADME properties. These results indicated that addition of nitro, carbamate, hydroxy, or fluoro moieties produced

Table 6. Anti-HIV activity of new DCK analogs in H9 and MT4 cell lines

Compound	H9 cell line[d]			MT-4 cell line[e]		
	$IC_{50}(\mu M)$[a]	$EC_{50}(\mu M)$[b]	SI[c]	IC_{50} (μM)	EC_{50} (μM)	SI
1a	>36.76	1.95	19	>73.53	2.94	25
2a	>32.93	1.62	>20	>65.88	0.24	>275
3a	>34.48	0.27	>128	>68.96	1.90	>36
3b	>21.58	0.0230	>938	>71.94	0.0905	>795
3c	34.67	0.0288	1205	>73.42	0.0808	>909
4a	>35.46	0.11	>322	>70.92	0.11	>645
4b	>37.04	0.0024	>15,433	>74.07	2.96	>25
4c	>37.82	0.0002	>189,100	>73.42	5.45	>13
5a	>33.88	1.50	>23	>67.75	39.60	>2
6a	>35.92	0.0522	>688	>71.84	0.00129	>55,690
7b	33.00	0.353	93	44.05	2.12	21
7c	22.73	0.0777	293	>71.94	0.0948	>759
8a	>35.64	1.80	>20	>71.28	2.85	>25
9a	>36.51	0.0175	>2,086	15.06	0.45	33
9b	>38.17	1.53	>25	N/A	N/A	N/A
AZT	1873.00	0.0168	111,488	>187.27	0.0055	>34,049

[a] Concentration that inhibits uninfected cell by 50%.
[b] Concentration that inhibits replication of virus by 50%.
[c] SI (selectivity index) = IC_{50}/EC_{50}.
[d] Assays in H9 lymphocytes were performed by Panacos Pharmaceuticals, Inc., Gaithersburg, Maryland, USA.
[e] Assays in the MT-4 cell line were performed by Beijing Institute of Microbiology & Epidemiology, Beijing, China.

Table 7. Comparison between experimental (H9) and predicted data of new DCK analogs

No.	Structure	pEC_{50}	CoMFA	CoMSIA	Log P
M02	4-Me-DCK[a]	2.23	2.195	2.141	5.09
M03	4-Me-5-MeO-DCK[a]	—	0.721	1.039	4.84
1a	3,4-di-Me-5-MeO-DCK	−0.470	0.450	0.741	5.12
2a	3-CH_2Br-4-Me-5-OMe-DCK	−0.210	0.326	0.453	5.32
3a	3-CH_2NO_2-4-Me-5-OMe-DCK	0.569	0.576	0.767	0.80
3b	3-CH_2NO_2-4-Me-DCK	1.638	1.663	1.803	1.06
3c	3-CH_2NO_2-DCK	1.541	1.407	1.835	0.90
4a	3-CH_2CN-4-Me-5-OMe-DCK	0.959	0.924	0.849	4.94
4b	3-CH_2CN-4-Me-DCK	2.620	1.622	1.745	5.19
4c	3-CH_2CN-DCK	3.699	1.778	1.640	5.04
5a	3-CH_2OAc-4-Me-5-OMe-DCK	−0.176	0.016	0.002	4.24
6a	3-CH_2OH-4-Me-5-OMe-DCK	1.282	2.246	1.883	4.11
7b	3-CH_2OCONH_2-4-Me-DCK	0.452	0.464	1.065	3.95
7c	3-CH_2OCONH_2-DCK	1.110	1.209	0.948	3.80
8a	3-Cl-4-Me-5-OMe-DCK	−0.255	0.754	0.184	4.74
9a	3-F-4-Me-5-OMe-DCK	1.745	0.453	0.246	4.36
9b	3-F-4-Me-DCK	−0.185	2.305	1.047	4.61

[a] Compounds published previously for comparison.

obvious changes in molecular physiochemical properties. The lower log *P* values (<5) of some new molecules suggest improved water solubility and lower lipophilicity. Such a change should not only improve molecular absorption but also decrease volumes of drug distribution in vivo, subsequently enhancing molecular oral bioavailability.

5. Conclusion

In conclusion, our current studies have established reliable CoMFA and CoMSIA models, which can efficiently guide further modification of DCK analogs. In addition, 15 new potent DCKs were designed, synthesized, and evaluated. Among these new structures, compounds **3b**, **3c**, **4b**, **4c**, **6a**, **7c**, and **9a** are potential anti-HIV drug candidates. In vivo evaluation and in silico ADME prediction studies are ongoing.

6. Experimental

6.1. General procedures

Melting points were measured with a RY-1 melting apparatus and are without correction. ^{1}H NMR spectra were measured on a JNM-ECA-400 spectrometer using TMS as internal standard. The solvent used was $CDCl_3$. Mass spectra were measured on a Perkin-Elmer Sciex API-3000 mass with Turbo Inospray ionization. Cario Arba Inc performed the elemental analyses on a Model-1106 analyzer. All target compounds were analyzed for C and H, and gave values within ±0.4% of the

theoretical values (see Table 8). Optical rotations were measured with a WZZ-T1 polarimeter at 25 °C at the sodium D line. The diastereoisomeric excess percentages were determined from the intensity of protons at the 3′- and 4′-positions in the ^{1}H NMR spectra. IR spectra were obtained with a Nicolet-550 Magna-IR spectrometer using KBr pellets. Silica gel GF_{245} and 200–400 mesh were purchased from Qingdao Haiyang Chemical Co., Ltd., for TLC, PTLC, and column chromatography. The Flash+ system from Biotage, Inc., was used for medium-pressure column chromatography. All other chemicals were obtained from Beijing Chemical Works or Aldrich, Inc.

6.1.1. (3′*R*,4′*R*)-3-Bromomethyl-3′,4′-di-*O*-(*S*)-camphanoyl-5-methoxy-4-methyl-(+)-*cis*-khellactone (2a). A mixture of 3,4-dimethyl-5-methoxyl-DCK (**1a**) (170 mg, 0.25 mmol) and *N*-bromosuccinimide (NBS, 0.26 mmol) in 5 mL of anhydrous benzene was refluxed for 3–4 h until the reaction was completed, as monitored by TLC (cyclohexane/EtOAc 6:4). The solvent was removed in vacuo. The residue was purified by silica gel chromatography (EtOAc/cyclohexane 3:7) to give 164 mg of **2a**. Yield: 86%, white solid, mp 159–162 °C; ^{1}H NMR δ ppm 0.97–1.11 (18H, ms, 6× CH_3), 1.43 and 1.49 (each 3H, s, CH_3), 1.66, 1.87, 2.20, and 2.50 (each 2H, m, CH_2), 2.63 (3H, s, CH_3-4), 3.90 (3H, s, CH_3O-5), 4.52 (2H, s, CH_2-3), 5.35 (1H, d,J = 4.8 Hz, H-3′), 6.29 (1H, s, H-6), 6.57 (1H, d, J = 4.8 Hz, H-4′); 87% de; MS (FAB+) *m*/*z* (%) 759 (M+1, 2), 761 (M+3, 2), 689 (M−Br, 35). IR (KBr) cm^{-1}: 3274, 1787 (C=O), 1735 (C=O), 1565 (benzene ring); Anal. ($C_{37}H_{43}BrO_{12}\cdot H_2O$) C, H.

6.1.2. General procedure for synthesizing 3-nitromethylated-DCKs (3a–3c). A mixture of 3-bromomethylated DCK analog (0.1 mmol) and sodium nitrite (0.12 mmol) in 2 mL DMF was stirred at room temperature until the reaction was completed, as monitored by TLC (cyclohexane/EtOAc 1:1). The mixture was poured into ice water and extracted with EtOAc (3× 20 mL). The combined organic layer was dried over Na_2SO_4 and the solvent was removed in vacuo. The residue was separated by PTLC (cyclohexane/EtOAc 6:4) to obtain a pure product.

6.1.3. (3′*R*,4′*R*)-3′,4′-Di-*O*-(*S*)-camphanoyl-5-methoxy-4-methyl-3-nitromethyl-(+)-*cis*-khellactone (3a). Yield: 33% (starting with 76 mg of **2a**); white solid, mp 162–164 °C; ^{1}H NMR δ ppm 0.97–1.11 (18H, overlapping s, 6× CH_3), 1.44 and 1.50 (each 3H, s, CH_3-2′), 1.63, 1.91, 2.22, and 2.50 (each 2H, m, CH_2), 2.63 (3H, s, CH_3-4), 3.89 (3H, s, CH_3O-5), 4.65 (2H, s, CH_2-3), 5.36 (1H, d, J = 4.8 Hz, H-3′), 6.29 (1H, s, H-6), 6.58 (1H, d, J = 4.8 Hz, H-4′); 85% de; MS (ESI$^+$) *m*/*z* (%) 714 (M−NO+NH4, 100), 679 (M−NO_2, 75); IR (KBr) cm^{-1}: 3098, 1787 (C=O), 1741 (C=O), 1570 (benzene ring), 1394 (NO_2); Anal. ($C_{37}H_{43}NO_{14}$) C, H, N.

Table 8. Elemental analysis data of new DCK analogs

Compound	Formula (MW)	Experimental (theoretical) (%)		
		C	H	N
1a	$C_{37}H_{44}O_{12}\cdot 1/4H_2O$	64.85	6.68	
	(685.25)	(64.79)	(6.54)	
2a	$C_{37}H_{43}BrO_{12}\cdot H_2O$	57.43	5.75	
	(777.65)	(57.15)	(5.83)	
3a	$C_{37}H_{43}NO_{14}$	61.04	6.09	2.02
	(725.74)	(61.23)	(5.97)	(1.93)
3b	$C_{36}H_{41}NO_{13}\cdot 2H_2O$	58.79	5.93	1.97
	(731.74)	(59.09)	(6.20)	(1.91)
3c	$C_{35}H_{39}NO_{13}\cdot 3H_2O$	57.32	6.49	1.98
	(735.73)	(57.14)	(6.16)	(1.90)
4a	$C_{38}H_{43}NO_{12}\cdot 4H_2O$	58.32	6.34	2.12
	(777.81)	(58.68)	(6.61)	(1.80)
4b	$C_{37}H_{41}NO_{11}\cdot 1/2H_2O$	64.98	6.50	
	(684.73)	(64.84)	(6.18)	
4c	$C_{36}H_{39}NO_{11}\cdot 5/4H_2O$	63.08	6.40	
	(684.21)	(63.19)	(6.11)	
5a	$C_{39}H_{46}O_{14}$	63.77	6.65	
	(738.77)	(63.40)	(6.28)	
6a	$C_{37}H_{44}O_{13}$	64.18	6.23	
	(696.75)	(63.78)	(6.37)	
7b	$C_{37}H_{43}NO_{13}\cdot H_2O$	61.16	6.15	2.05
	(727.75)	(61.06)	(6.23)	(1.92)
7c	$C_{36}H_{41}NO_{13}\cdot 2H_2O$	59.38	5.91	2.08
	(731.74)	(59.09)	(6.20)	(1.91)
8a	$C_{36}H_{41}ClO_{12}\cdot H_2O$	59.86	6.00	
	(719.18)	(60.12)	(6.03)	
9a	$C_{36}H_{41}FO_{12}\cdot 1/2H_2O$	61.97	5.98	
	(693.71)	(62.33)	(6.10)	
9b	$C_{35}H_{39}FO_{11}$	63.95	6.32	
	(655.41)	(64.21)	(6.00)	

6.1.4. (3′*R*,4′*R*)-3′,4′-Di-*O*-(*S*)-camphanoyl-4-methyl-3-nitromethyl-(+)-*cis*-khellactone (3b). Yield: 34.4% (starting with 146 mg of **2b**); white solid, mp 157–161 °C; ^{1}H NMR δ ppm 0.97–1.12 (18H, ms, 6× CH_3), 1.45 and 1.49 (each 3H, s, CH_3-2′), 1.68, 1.93, 2.23, and 2.47 (each 2H, m, CH_2), 2.50 (3H, s, CH_3-4), 4.66 (2H, s, CH_2-3), 5.39 (1H, d, J = 4.8 Hz, H-3′), 6.65 (1H, d, J = 4.8 Hz, H-4′), 6.87 (1H, d, J = 8.8 Hz, H-6), 7.62 (1H, d, J = 8.8 Hz, H-5); 89% de; MS (ESI$^+$) *m*/*z* (%) 689 (M−NO+Na, 100), 684 (M−NO+NH_4, 50), 649 (M−NO_2, 40); IR (KBr) cm^{-1}: 3399, 2970, 2480, 1798 (C═O), 1750 (C═O), 1600 (benzene ring), 1386 (NO_2); Anal. ($C_{36}H_{41}NO_{13}$·2H_2O) C, H, N.

6.1.5. (3′*R*,4′*R*)-3′,4′-Di-*O*-(*S*)-camphanoyl-3-nitromethyl-(+)-*cis*-khellactone (3c). Yield: 44% (starting with 107 mg of **2b**); white solid, mp 137–139 °C; ^{1}H NMR δ ppm 0.98–1.11 (18H, ms, 6× CH_3), 1.45 and 1.49 (each 3H, s, CH_3-2′), 1.63, 1.92, 2.23, and 2.49 (each 2H, m, CH_2), 4.56 (2H, s, CH_2-3), 5.40 (1H, d, J = 4.8 Hz, H-3′), 6.65 (1H, d, J = 4.8 Hz, H-4′), 6.85 (1H, d, J = 8.8 Hz, H-6), 7.42 (1H, d, J = 8.8 Hz, H-5), 7.67 (1H, s, H-4); 90% de; MS (ESI$^+$) *m*/*z* (%): 675 [(M+1)−NO+Na, 21], 670 [(M+1)−NO+ NH_4, 37], 653 (M−NO_2+ NH_4, 100), 635 (M−NO_2, 79). IR (KBr) cm^{-1}: 3398, 2974, 1798 (C═O),1741 (C═O), 1570 (benzene ring), 1415; Anal. ($C_{35}H_{39}NO_{13}$·3H_2O) C, H, N.

6.1.6. General procedure for synthesizing 3-cyanomethylated-DCKs. A mixture of 3-bromomethyl-DCK analog (0.5 mmol) and sodium cyanide (0.6 mmol) in 1 mL DMSO was heated to 60 °C (oil bath) for 4 h until the reaction was complete, as monitored by TLC (cyclohexane/EtOAc 6:4). The mixture was then cooled to room temperature, poured into ice water, and extracted with EtOAc (3× 25 mL). The organic layer was dried over $MgSO_4$ and the solvent was removed in vacuo. The residue was separated by PTLC (cyclohexane/EtOAc 6:4) to give a pure product.

6.1.7. (3′*R*,4′*R*)-3′,4′-Di-*O*-(*S*)-camphanoyl-3-cyanomethyl-5-methoxy-4-methyl-(+)-*cis*-khellactone (4a). Yield: 85% (starting with 38 mg of **2b**), white solid, mp 165–167 °C; ^{1}H NMR δ ppm 0.97–1.12 (18H, overlapping s, 6× CH_3), 1.43 and 1.49 (each 3H, s, CH_3-2′), 1.70, 1.92, 2.20, and 2.49 (each 2H, m, 4× CH_2), 2.68 (3H, s, CH_3-4), 3.71 (2H, s, CH_2-3), 3.91 (3H, s, CH_3O-5), 5.36 (1H, d, J = 4.8 Hz, H-3′), 6.31 (1H, s, H-6), 6.56 (1H, d, J = 4.8 Hz, H-4′); 86% de; MS (ESI$^+$) *m*/*z* (%) 706 (M+1, 40); IR (KBr) cm^{-1}: 3026, 1787 (C═O), 1726 (C═O), 1575 (benzene ring), 1404; Anal. ($C_{38}H_{43}NO_{12}$·4H_2O) C, H, N.

6.1.8. (3′*R*,4′*R*)-3′,4′-Di-*O*-(*S*)-camphanoyl-3-cyanomethyl-4-methyl-(+)-*cis*-khellactone (4b). Yield: 49% (starting with 146 mg of **2b**), white solid, mp158–160 °C, ^{1}H NMR δ ppm 0.98–1.12 (18H, overlapping s, 6× CH_3), 1.46 and 1.49 (each 3H, s, CH_3-2′), 1.69, 1.93, 2.23, and 2.50 (each 2H, m, 4× CH_2), 2.53 (3H, s, CH_3-4), 3.72 (2H, s, CH_2-3), 5.40 (1H, d, J = 4.8 Hz, H-3′), 6.64 (1H, d, J = 4.8 Hz, H-4′), 6.89 (1H, d, J = 8.8 Hz, H-6), 7.62 (1H, d, J = 8.8 Hz, H-5); 75% de; MS (ESI) *m*/*z* (%) 698 (M+Na$^+$, 100), 693 (M+NH4$^+$, 100), 676 (M$^+$+1, 10); [α]$_D$ +24.88 (*c* 1.474, $CHCl_3$). IR (KBr) cm^{-1}: 2972, 2935, 1793 (C═O), 1766 (C═O), 1722 (C═O), 1595 (benzene ring), 1407; Anal. ($C_{37}H_{41}NO_{11}$·1/2 H_2O) C, H.

6.1.9. (3′*R*,4′*R*)-3′,4′-Di-*O*-(*S*)-camphanoyl-3-cyanomethyl-(+)-*cis*-khellactone (4c). Yield: 21% (starting with 107 mg of **2b**), white solid, mp130–133 °C, ^{1}H NMR δ ppm 0.98–1.45 (24H, overlapping s, each 3H, 8× CH_3), 1.68, 1.93, 2.22, and 2.50 (each 2H, m, 4× CH_2), 4.56(2H, s, CH_2-3), 5.40 (1H, d, J = 4.8 Hz, H-3′), 6.66 (1H, d, J = 4.8 Hz, H-4′), 6.84 (1H, d, J = 8.8 Hz, H-6), 7.43 (1H, d, J = 8.8 Hz, H-5), 7.67 ((1H, s, H-4); 90% de; MS (ESI) *m*/*z* (%) 653 [(M−CN)+NH_4^+, 67], 636 [(M−CN)+1$^+$, 98], 455 (100); IR (KBr) cm^{-1}: 3409, 2974, 2932, 1788 (C═O), 1735 (C═O), 1565 (benzene ring), 1410; Anal. ($C_{36}H_{39}NO_{11}$·1 1/4H_2O) C, H.

6.1.10. (3′*R*,4′*R*)-3-Acetoxymethyl-3′,4′-di-*O*-(*S*)-camphanoyl-5-methoxy-4-methyl-(+)-*cis*-khellactone (5a). A mixture of **2a** (144 mg, 0.19 mmol) and NaOAc (19 mg) in 3 mL of acetic anhydride was refluxed for 3 h and monitored by TLC (cyclohexane/EtOAc 6:4). The mixture was cooled to room temperature, poured into ice water, and allowed to stand overnight. The precipitated **5a** was filtered, washed with water until neutral, and dried to obtain a white solid (93 mg, yield 66%). mp 165–166 °C; ^{1}H NMR δ ppm 0.97–1.11 (18H, overlapping s, 6× CH_3), 1.43 and 1.49 (each 3H, s, CH_3-2′), 1.68, 1.92, 2.23, and 2.50 (each 2H, m, CH_2), 2.06 (3H, s, CH_3CO), 2.60 (3H, s, CH_3-4), 3.92 (3H, s, CH_3O-5), 5.12 (2H, s, CH_2-3), 5.36 (1H, d,J = 4.8 Hz, H-3′), 6.28 (1H, s, H-6), 6.56 (1H, d,J = 4.8 Hz, H-4′); 82% de; MS (FAB+) *m*/*z* (%) 738 (M, 12); IR (KBr) cm^{-1}: 3400, 1788 (C═O), 1736 (C═O), 1570 (benzene ring), 1404; Anal. ($C_{39}H_{46}O_{14}$) C, H.

6.1.11. (3′*R*,4′*R*)-3′,4′-Di-*O*-(*S*)-camphanoyl-3-hydroxymethyl-5-methoxy-4-methyl-(+)-*cis*-khellactone (6a). A solution of **5a** (46 mg, 0.06 mmol) in EtOH (3 mL) containing a few drops of aqueous HCl (10%) was refluxed for 1 h. The mixture was cooled, poured into ice water, and allowed to stand overnight. The white solid was collected and washed with water until neutral. The crude product was purified by PTLC (EtOAc/cyclohexane 1:1) to give 28 mg of **6a** as a white solid. Yield: 52%, mp 158–160 °C; ^{1}H NMR δ ppm 0.97–1.34 (18H, overlapping s, 6× CH_3), 1.43 and 1.49 (each 3H, s, CH_3-2′), 1.70, 1.92, 2.20, and 2.49 (each 2H, m, 4× CH_2), 2.63 (3H, s, CH_3-4), 3.89 (3H, s, CH_3O-5), 4.65 (2H, s, CH_2-3), 5.36 (1H, d, J = 4.8 Hz, H-3′), 6.31 (1H, s, H-6), 6.58 (1H, d,J = 4.8 Hz, H-4′); 91% de; MS (ESI+) *m*/*z* (%) 719 (M+Na, 100), 714 (M+NH_4, 53); IR (KBr) cm^{-1}: 3399, 2964, 2767, 1792 (C═O), 1736 (C═O), 1715 (C═O), 1575 (benzene ring), 1399; Anal. ($C_{37}H_{44}O_{13}$) C, H.

6.1.12. (3′*R*,4′*R*)-3′,4′-Di-*O*-(*S*)-camphanoyl-3-hydroxymethyl-4-methyl-(+)-*cis*-khellactone (6b) and (3′*R*,4′*R*)-3′,4′-di-*O*-(*S*)-camphanoyl-3-hydroxymethyl-(+)-*cis*-khellactone (6c). The synthetic methodology was identical to

that described for **6a** and both compounds were described previously.[6]

6.1.13. (3′*R*,4′*R*)-3′,4′-Di-*O*-(*S*)-camphanoyl-3-carbamoyloxymethyl-4-methyl-(+)-*cis*-khellactone (7b). A solution of **6b** (67 mg, 0.1 mmol) in CH_2Cl_2 (5 mL) was added to a solution of *p*-nitrophenyl chloroformate in CH_2Cl_2 (5 mL) at 0 °C over 0.5 h. TLC (cyclohexane/EtOAc 1:1) was used to monitor the reaction. The mixture was diluted with EtOAc and washed successively with aqueous HCl (10%), saturated sodium bicarbonate, and brine until neutral. The organic solvent was removed in vacuo and, without further purification, the solid residue was dissolved in THF (15 mL), cooled to 0 °C, and treated with aqueous ammonia (1mL). After stirring for 3 h, the yellow solution was diluted with EtOAc (100 mL) and washed successively with water, saturated sodium bicarbonate, and brine. After the solvent was removed in vacuo, the residue was purified by PTLC (EtOAc/cyclohexane 1:1) to afford 60 mg of **7b**, yield 85%, white solid, mp 147–149 °C; ^{1}H NMR δ ppm 0.97–1.12 (18H, overlapping s, 6× CH_3), 1.45 and 1.49 (each 3H, s, CH_3-2′), 1.70, 1.90, 2.23, and 2.50 (each 2H, m, CH_2), 2.52 (3H, s, CH_3-4), 4.66 (2H, br., NH_2), 5.15 (2H, s, CH_2-3), 5.40 (1H, d, J = 4.8 Hz, H-3′), 6.63 (1H, d, J = 4.8 Hz, H-4′), 6.86 (1H, d, J = 8.8 Hz, H-6), 7.62 (1H, d, J = 8.8 Hz, H-6); 91 %de; MS (ESI$^+$) *m*/*z* (%) 727 (M+NH_4, 100), 710 (M+1, 8); IR (KBr) cm^{-1}: 3430, 2984, 1782 (C═O), 1726 (C═O), 1575 (benzene ring), 1399; Anal. ($C_{37}H_{43}NO_{13}\cdot H_2O$) C, H, N.

6.1.14. (3′*R*,4′*R*)-3′,4′-Di-*O*-(*S*)-camphanoyl-3-carbamoyloxymethyl-(+)-*cis*-khellactone (7c). Compound **6c** was treated identically to **6b** above to afford **7c** in 56% yield as a white solid. mp 122–124 °C; ^{1}H NMR δ ppm 0.97–1.12 (18H, overlapping s, 6× CH_3), 1.45 and 1.49 (each 3H, s, CH_3-2′), 1.70, 1.90, 2.23, and 2.50 (each 2H, m, CH_2), 4.73 (2H, br. NH_2), 5.00 (2H, s, CH_2-3), 5.40 (1H, d, J = 4.8 Hz, H-3′), 6.64 (1H, d, J = 4.8 Hz, H-4′), 6.83 (1H, d, J = 8.8 Hz, H-6), 7.43 (1H, d, J = 8.8 Hz, H-5), 7.72 (1H, s, H-4); 78.8% de; MS (ESI$^+$) *m*/*z* (%) 713 (M+NH_4, 60), 696 (M+1, 20); IR (KBr) cm^{-1}: 3420, 2808, 1788 (C═O), 1736 (C═O), 1570 (benzene ring), 1404; Anal. ($C_{36}H_{41}NO_{13}\cdot 2H_2O$) C, H, N.

6.1.15. 3,4-Dimethyl-5-methoxy-3′,4′-dihydroseselin (24). $NaBH_4$ (4.60 g, 122 mmol) was added to a mixture of **23** (5.33 g, 24 mmol) in toluene (60 mL) and 10% KOH aq (100 mL). The mixture was refluxed for 4 h with monitoring by TLC (cyclohexane/EtOAc 7:3). After cooling to room temperature, the reaction mixture was poured into ice water, acidified with 10% aq HCl until neutral, extracted with Et_2O three times, washed with brine, and dried. After removing the solvent in vacuo, the residue in anhydrous CH_2Cl_2 (25 mL) was reacted with ethyl acetoacetate (3.3 mL, 26 mmol) in the presence of $BF_3\cdot EtO_2$ (1 mL) under N_2 at room temperature for 29 h. Then, the mixture was poured into ice water and extracted with CH_2Cl_2 three times. The solvent was removed in vacuo, and the residue was purified by silica gel chromatography (cyclohexane/EtOAc 2:8) to give 3.54 g of **24** in a yield of 50%, pale yellow solid, mp 141–143 °C; ^{1}H NMR δ ppm 1.36 (6H, s, 2× CH_3-2′), 1.83 (2H, t, J = 6.8 Hz, CH_2-3′), 2.16 (3H, s, CH_3-3), 2.55 (3H, s, CH_3-4), 2.81 (2H, t, J = 6.8 Hz, CH_2-4′), 3.82 (3H, s, CH_3O-5), 6.22 (1H, s, H-6); MS (ESI+) *m*/*z* (%) 289 (M+1, 100).

6.1.16. 3-Chloro-5-methoxy-4-methyl-3′4′-dihydroseselin (25). Compound **23** (1.11 g, 5 mmol) was first treated with $NaBH_4$ as described above for **24**, and the crude intermediate was reacted with ethyl 2-chloroacetoacetate (0.83 mL, 6 mmol) for 24 h to give 766 mg of **25**, yield 53%, white solid, mp 173–176 °C; ^{1}H NMR δ ppm 1.36 (6H, s, 2× CH_3-2′), 1.83 (2H, t, J = 6.8 Hz, CH_2-3′), 2.74 (3H, s, CH_3-4), 2.80 (2H, t, J = 6.8 Hz, CH_2-4′), 3.84 (3H, s, CH_3O-5), 6.27 (1H, s, H-6); MS (ESI+) *m*/*z* (%) 309 (M+1, 100), 311 (M+3, 33).

6.1.17. 3-Fluoro-5-methoxy-4-methyl-3′4′-dihydroseselin (26). As in the preparation of **25**, compound **23** (444 mg, 2 mmol) was reacted with $NaBH_4$ and then with ethyl 2-fluoroacetoacetate (373 mg, 2.5 mmol) to afford 383 mg of **26**, yield 66%, white solid, mp 157–160 °C; ^{1}H NMR δ ppm 1.56 (6H, s, 2× CH_3-2′), 1.83 (2H, t, J = 6.8 Hz, CH_2-3′), 2.52 (3H, s, CH_3-4), 2.80 (2H, t, J = 6.8 Hz, CH_2-4′), 3.83 (3H, s, CH_3O-5), 6.28 (1H, s, ArH-6); MS (ESI+) *m*/*z* (%) 293 (M^++1, 100).

6.1.18. 3,4-Dimethyl-5-methoxyseselin (27). A solution of **24** (1.73 g, 6 mmol) in 1,4-dioxane (40 mL) was added dropwise to a solution of DDQ (3.78 g, 14 mmol) in anhydrous 1,4-dioxane (60 mL) over 1 h under N_2 at room temperature. The darkened reaction mixture was then heated to reflux for 12 h. After cooling, the solvent was removed in vacuo. The residue was dissolved in CH_2Cl_2, passed through a short column of silica (60–100 mesh), and then washed with CH_2Cl_2 to obtain **27** (247 mg, yield 14%), a pale yellow solid, mp 173–175 °C; ^{1}H NMR δ ppm 1.45 (6H, s, 2× CH_3-2′), 2.15 (3H, s, CH_3-3), 2.53 (3H, s, CH_3-4), 3.85 (3H, s, CH_3O-5), 5.56 (1H, d, J = 8.8 Hz, H-3′), 6.26 (1H, s, H-6), 6.85 (1H, d, J = 8.8 Hz, H-4′); MS (ESI+) *m*/*z* (%) 287 (M+1, 100).

6.1.19. 3-Chloro-5-methoxy-4-methylseselin (28). Compound **28** was prepared identical to the synthesis of **27**. Yield: 31% (starting with 308 mg of **25**), white solid, mp 200–202 °C; ^{1}H NMR δ ppm 1.46 (6H, s, 2× CH_3-2′), 2.73 (3H, s, CH_3-4), 3.87 (3H, s, CH_3O-5), 5.59 (1H, d, J = 8.8 Hz, H-3′), 6.30 (1H, s, H-6), 6.81 (1H, d, J = 8.8 Hz, H-4′); MS (ESI$^+$) *m*/*z* (%) 307 (M+1, 100), 309 (M+3, 35).

6.1.20. 3-Fluoro-5-methoxy-4-methylseselin (29). As in the synthesis of **27**, a mixture of **26** (440 mg, 1.5 mmol) and DDQ (excess) in anhydrous THF was refluxed for 16 h to afford 310 mg of **29**, white solid, yield 67%. mp 195–197 °C; ^{1}H NMR δ ppm 1.45 (6H, s, 2× CH_3-2′), 2.52 (3H, s, CH_3-4), 3.86 (3H, s, CH_3O-5), 5.59 (1H, d, J = 8.8 Hz, H-3′), 6.30 (1H, s, H-6), 6.79 (1H, d, J = 8.8 Hz, H-4′); MS (ESI+) *m*/*z* (%) 291 (M+1, 100).

6.1.21. 3-Fluoro-7-hydroxy-4-methylcoumarin (30). To a mixture of resorcinol (330 mg, 3 mmol) and ethyl 2-fluoroacetoacetate (0.4 mL, 3.2 mmol) was slowly added 98%H_2SO_4(2–3 mL, excess)with stirring at 0 °C for over 1 h. Then, the mixture was stirred at rt for 3 h, poured into ice water, and allowed to stand overnight. The precipitated solid was filtered and washed with water until neutral. After drying in vacuo, **30** was obtained as a white solid (422 mg). Yield: 73.4%, mp 163–165 °C; ^{1}H NMR δ ppm 2.39 (3H, s, CH_3-4), 6.80 (1H, d, J = 2.6 Hz, H-8), 6.94 (1H, dd, J = 2.6 and 8.8 Hz, H-6), 7.61 (1H, d, J = 8.8 Hz, H-5), 9.34 (1H, s, OH-7).

6.1.22. 3-Fluoro-4-methylseselin (31). A mixture of 3-fluoro-7-hydroxy-4-methylcoumarin (**30**) (400 mg, 2.1 mmol), K_2CO_3 (724 mg, 5.25 mmol), KI (348 mg, 2.1 mmol), and 3-chloro-3-methyl-1-butyne (1–2 mL, excess) in DMF (10 mL) was heated to 70–80 °C with stirring until the reaction was complete, as monitored by TLC. K_2CO_3 was filtered and the filtrate was concentrated in vacuo. Without purification, the residue was heated to reflux in 10 mL *N*,*N*-diethylaniline for 4–6 h. The mixture was cooled to rt, diluted with EtOAc, and washed with 10% HCl aq, water, and brine, successively. After removing the organic solvent in vacuo, the residue was purified by column chromatography with an eluant of cyclohexane/EtOAc 7:3 to afford 97.5 mg of **31**, white solid, yield 18%, mp 120–125 °C; ^{1}HNMR δ ppm 1.47 (6H, s, 2× CH_3-2′), 2.36 (3H, s, CH_3-4), 5.76 (1H, d, J = 10.2 Hz, H-3′), 6.82 (1H, d, J = 8.8 Hz, H-6), 6.88 (1H, d, J = 10.2 Hz, H-4′), 7.31 (1H, d, J = 8.8 Hz, H-5).

6.1.23. General procedure of asymmetric dihydroxylation and esterification to synthesize substituted (3′*R*,4′*R*)-3′,4′-di-*O*-(*S*)-camphanoyl-(+)-*cis*-khellactone analogs from corresponding substituted seselins. Details were described in Ref. 17.

6.1.24. (3′*R*,4′*R*)-3′,4′-Di-*O*-(*S*)-camphanoyl-3,4-dimethyl-5-methoxy-(+)-*cis*-khellactone (1a). Yield: 73% (starting with 343 mg of **27**), white solid, mp 171–172 °C, purified with PTLC (silica gel, cyclohexane/EtOAc 7:3); ^{1}H NMR δ ppm 0.95–1.09 (18H, overlapping s, 6× CH_3), 1.43 and 1.49 (each 3H, s, CH_3-2′), 1.65 and1.90 (each 2H, m, CH_2), 2.08 (3H, s, CH_3-3), 2.20 and 2.38 (each 2H, m, CH_2), 2.49 (3H, s, CH_3-4), 3.86 (3H, s, CH_3O), 5.33 (1H, d, J = 4.8 Hz, H-3′), 6.25 (1H, s, H-6), 6.53 (1H, d, J = 4.8 Hz, H-4′); 87% de; MS (FAB+) m/z (%) 680 (M, 5), 483 (M−197,100); IR (KBr) cm^{-1}: 3098, 2984, 1793 (C═O), 1756 (C═O), 1715 (C═O); Anal. ($C_{37}H_{44}O_{12}$·1/4H_2O) C, H.

6.1.25. (3′*R*,4′*R*)-3′,4′-Di-*O*-(*S*)-camphanoyl-3-chloro-5-methoxy-4-methyl-(+)-*cis*-khellactone (8a). Yield: 38% (starting with 61 mg of **28**), purified with PTLC (silica gel, cyclohexane/EtOAc 7:3), white solid, mp 243–245 °C; ^{1}H NMR δ ppm 0.97–1.12 (18H, overlapping s, 6× CH_3), 1.44 and 1.49 (each 3H, s, CH_3-2′), 1.66, 1.87, 2.20, and 2.50 (each 2H, m, CH_2), 2.74 (3H, s, CH_3-4), 3.90 (3H, s, CH_3O-5), 5.36 (1H, d, J = 4.8 Hz, H-3′), 6.31 (1H, s, H-6), 6.55 (1H, d, J = 4.8 Hz, H-4′); 84% de; MS (ESI$^+$) m/z (%) 718 (M+NH_4, 100), 720 [(M+2)+NH_4, 30]; IR (KBr) cm^{-1}: 3420, 2808, 1788 (C═O), 1741 (C═O), 1570 (benzene ring), 1404; Anal. ($C_{36}H_{41}ClO_{12}$·H_2O) C, H.

6.1.26. (3′*R*,4′*R*)-3′,4′-Di-*O*-(*S*)-camphanoyl-3-fluoro-5-methoxy-4-methyl-(+)-*cis*-khellactone (9a). Yield: 35% (starting with 58 mg of **29**), purified with PTLC (silica gel, cyclohexane/EtOAc 7:3), white solid, mp 169–171 °C; ^{1}H NMR δ ppm 0.97–1.11 (18H, overlapping s, 6× CH_3), 1.44 and 1.48 (each 3H, s, CH_3-2′), 1.70, 1.94, 2.22, and 2.48 (each 2H, m, CH_2), 2.53 (3H, s, CH_3-4), 3.89 (3H, s, CH_3O-5), 5.36 (1H, d, J = 4.8 Hz, H-3′), 6.31 (1H, s, H-6), 6.55 (1H, d, J = 4.8 Hz, H-4′); 84% de; MS (ESI+) *m*/*z* (%) 702 (M+NH_4, 100); IR (KBr) cm^{-1}: 3285, 1788 (C═O), 1746 (C═O), 1570 (benzene ring), 1404; Anal. ($C_{36}H_{41}FO_{12}$·1/2H_2O) C, H.

6.1.27. (3′*R*,4′*R*)-3′,4′-Di-*O*-(*S*)-camphanoyl-3-fluoro-4-methyl-(+)-*cis*-khellactone (9b). Yield: 80% (starting with 650 mg of **31**), purified with PTLC (silica gel, cyclohexane/EtOAc 7:3), white solid, mp 156–160 °C; ^{1}H NMR δ ppm 0.99–1.11 (18H, overlapping s, 6× CH_3), 1.42 and 1.51 (each 3H, s, CH_3-2′), 1.55, 2.05, 2.18, and 2.53 (each 2H, m, CH_2), 2.43 (3H, s, CH_3-4), 5.49 (1H, d, J = 4.8 Hz, H-3′), 6.71 (1H, d, J = 4.8 Hz, H-4′), 7.02 (1H, d, J = 8.8 Hz, H-6), 7.02 (1H, d, J = 8.8 Hz, H-5); 84% de; MS (ESI$^+$) *m*/*z* (%) 655.4 (M, 100), 457 (M−198, 80); IR (KBr) cm^{-1}: 3420, 2964, 1782 (C═O), 1751 (C═O), 1559 (benzene ring), 1410; Anal. ($C_{35}H_{39}FO_{11}$) C, H.

6.2. HIV growth inhibition assay in H9 lymphocytes

The human T-cell line, H9, was maintained in continuous culture with complete medium (RPMI 1640 with 10% fetal calf serum supplemented with L-glutamine at 5% CO_2 and 37 °C. Test samples were prepared, as described previously,[6] and to each sample well were added 90 μL of media containing H9 cells at 3×10^5 cells/mL and 45 μL of virus inoculum (HIV-1 IIIIB isolate) containing 125 $TCID_{50}$. Control wells containing virus and cells only (no drug) and cells only (no virus or drug) were also prepared. A second set of samples was prepared identical to the first and added to cells under identical conditions without virus (mock infection) for toxicity determinations (IC_{50} defined below). In addition, AZT was also assayed during each experiment as a positive drug control. On days 1 and 4 post-infection (PI), spent media were removed from each well and replaced with fresh media. On day 6 PI, the assay was terminated and culture supernatants were harvested for analysis of virus replication by p24 antigen capture. The compound toxicity was determined by XTT using the mock-infected sample wells. If a test sample inhibited virus replication and was not toxic, its effects were reported in the following terms: IC_{50}, the concentration of the test sample that was toxic to 50% of the mock-infected cells; EC_{50}, the concentration of the test sample that was able to suppress HIV replication by 50%; and the selectivity index (SI), the ratio of the IC_{50} to EC_{50}.

6.3. HIV growth inhibition assay in the MT4 cell line

The human T-cell line, MT-4, was maintained in continuous culture with complete medium (RPMI 1640 with 10% fetal calf serum supplemental with L-glutamine) at 5% CO_2 and 37 °C. Test samples were dissolved in medium and the following final drug concentrations were routinely used for screening: 200, 40, 8, 1.6, 0.32, 0.064, 0.0128, and 0.00256 μg/mL. Fifty microliters of each test sample was added to the 96-well cell culture plate and to each well were added 50 μL of media containing MT-4 cells at 8×10^4 cells/mL and 100 μL of virus supernatant (HIV-1 IIIB isolate) containing 100 $TCID_{50}$. Control wells containing virus and cells only (no drug) and cells only (no virus or drug) were also prepared. An identical second set of samples was prepared and 100 μL of each was added to the well mixed with 100 μL MT-4 cells under identical conditions without virus (mock infection) for toxicity determinations (IC_{50}). In addition, AZT was also assayed during each experiment as a positive drug control. On day 4 post-infection (PI), culture supernatants were removed from each well and replaced with fresh media. On day 7 PI, the assay was terminated and 20 μL of 5% MTT was added to each well. After 4 h, supernatant was removed from each well after centrifuging for 5 min. Afterwards, 100 μL dimethylsulfoxide (DMSO) that can be dissolved was added to each well. Results were read by a microplate reader and reported as IC_{50}, EC_{50}, and selectivity index (SI).

Acknowledgments

This investigation was supported by Grant 30271544 from the National Natural Science Foundation of China (NSFC) awarded to L. Xie, and in part by Grant AI-33066 from the National Institute of Allergy and Infectious Diseases awarded to K. H. Lee.

References and notes

1. Huang, L.; Kashiwada, Y.; Cosentino, L. M.; Fan, S.; Lee, K. H. *Bioorg. Med. Chem. Lett.* **1994**, *4*, 593.
2. Yu, D.; Suzuki, M.; Xie, L.; Morris-Natschke, S. L.; Lee, K. H. *Med. Res. Rev.* **2003**, *23*, 322.
3. Huang, L.; Kashiwada, Y.; Cosentino, L. M.; Fan, S.; Chen, C. H.; McPhail, A. T.; Fujioka, T.; Mihashi, K.; Lee, K. H. *J. Med. Chem.* **1994**, *37*, 3947.
4. Xie, L.; Takeuchi, Y.; Cosentino, L. M.; Lee, K. H. *J. Med. Chem.* **1999**, *42*, 2662.
5. Xie, L.; Takeuchi, Y.; Cosentino, L. M.; McPhail, A. T.; Lee, K. H. *J. Med. Chem.* **2001**, *44*, 664.
6. Xie, L.; Yu, D.; Wild, C.; Allaway, G.; Turpin, J.; Smith, P.; Lee, K. H. *J. Med. Chem.* **2004**, *47*, 756.
7. Xie, L.; Takeuchi, Y.; Cosentino, L. M.; Lee, K. H. *Bioorg. Med. Chem. Lett.* **1998**, *8*, 2151.
8. Chen, H. F.; Yao, X. J.; Li, Q.; Yuan, S. G.; Panaye, A.; Doucet, J. P.; Fan, B. T. *SAR QSAR Environ. Res.* **2003**, *14*, 455.
9. Chen, H. F.; Li, Q.; Yao, X. J.; Fan, B. T.; Yuan, S. G.; Panaye, A.; Doucet, J. P. *QSAR Comb. Sci.* **2003**, *22*, 604.
10. Chen, H. F.; Li, Q.; Yao, X. J.; Fan, B. T.; Yuan, S. G.; Panaye, A.; Doucet, J. P. *QSAR Comb. Sci.* **2004**, *23*, 36.
11. SYBYL[Computer Program]. Version 6.9, St. Louis(MO): Tripos Associates Inc., 2002.
12. Clark, M.; Cramer, R. D., III; Van Opdenbosh, N. *J. Comput. Chem.* **1989**, *10*, 982.
13. Cho, S. J.; Tropsha, A. *J. Med. Chem.* **1995**, *38*, 1060.
14. Clark, M.; Cramer, R. D., III *Quant. Struct.-Act. Relat.* **1993**, *12*, 137.
15. Klebe, G.; Abraham, U.; Mietzner, T. *J. Med. Chem.* **1994**, *37*, 4130.
16. Böhm, M.; Stürzebecher, J.; Klebe, G. *J. Med. Chem.* **1999**, *42*, 458.
17. Leach, A. R. *Molecular modelling principles and applications*; Henry Ling Ltd: London, 2001, pp 695–702.
18. Paz, M. M.; Sardina, F. J. *J. Org. Chem.* **1993**, *58*, 6990.
19. Schuda, P. F.; Price, W. A. *J. Org. Chem.* **1987**, *52*, 1972.
20. Xie, L.; Crimmins, M. T.; Lee, K. H. *Tetrahedron Lett.* **1995**, *36*, 4529.
21. Yu, D.; Chen, C. H.; Brossi, A.; Lee, K. H. *J. Med. Chem.* **2004**, *47*, 4072.